Physica Medica 62 (2019) 33–40

Contents lists available at ScienceDirect

Physica Medica

journal homepage: www.elsevier.com/locate/ejmp

Original paper

Improving individualised dosimetry in radioiodine therapy for hyperthyroidism using population biokinetic modelling

J. Melgar Pérez[a,*], A. Orellana Salas[a], Y. Santaella Guardiola[b], J.C. Antoranz Callejo[c]

[a] UGC Radiofísica, Servicio de Radiofísica y Protección Radiológica, Hospital Punta de Europa, 11207 Algeciras (Cádiz), Spain
[b] Servicio de Medicina Nuclear, Hospital Punta de Europa, 11207 Algeciras (Cádiz), Spain
[c] UNED, Departamento de Física Matemática y de Fluidos, 28040 Madrid, Spain

ARTICLE INFO

Keywords:
Radioiodine dosimetry
Hyperthyroidism
Nonlinear mixed-effects model
Population biokinetics
Individualised dosimetry

ABSTRACT

The application of an individualised dosimetric procedure for radioiodine therapy requires the intensive use of resources in nuclear medicine facilities. In practice, the amount of data taken per patient is too limited to obtain an accurate estimate of the absorbed dose in the thyroid. The individualised absorbed dose estimates can be enhanced using statistical tools for population-based approaches. The aim of this work was to build a population biokinetic model of thyroid uptake and elimination of radioiodine using a nonlinear mixed-effects approach in patients with Graves' disease. Input data for the model development were taken from a dosimetric method based on ^{123}I imaging data. ^{123}I decay-corrected uptake values were estimated at 4, 24, and 96 h post-administration and for 58 patients. The root mean squared error (RMSE) for predicted ^{123}I uptake values by the fitted model was 4%. The root mean squared error of prediction (RMSEP) for out-of-sample ^{123}I uptake values, computed by a leave-one-out cross-validation, was 12%. We calculated ^{131}I activity to administer from out-of-sample predicted ^{123}I uptake values and compared the result with that calculated from observed ^{123}I uptake values. RMSEP values for therapeutic activity revealed that there were measuring points with higher weight than others in the model. The mixed-effects approach can be used to enhance the accuracy of dosimetric calculations in therapies using ^{131}I. Assessing the accuracy of the predictive model enables choosing among different time-sampling schedules of the radioiodine thyroid uptake curve. This methodology can also be applied in other areas of radiation dosimetry.

1. Introduction

Radioiodine (^{131}I) therapy has been used for the management of hyperthyroidism for more than 70 years. Despite the history of using radioiodine for hyperthyroidism, there are no conclusive studies regarding the optimal procedure to be administered to patients in order to achieve an optimal absorbed dose to the thyroid gland and a resulting optimal clinical outcome [1].

The most common approach followed in clinical practice is the administration of a fixed and generally high activity for all patients [2]. The implementation of an individualised dosimetric method is not carried out for several reasons. First, the estimation of the thyroid absorbed dose with some accuracy is a complex problem that requires additional resources and is time-consuming, so it is not considered cost-effective [1]. Second, the administration of high activities induces hypothyroidism, which is not considered a problem, as it is treated with life-long hormonal replacement therapy [1]. Third, many clinical studies have not shown that clinical efficacy is enhanced using individualised dosimetric approaches [1]. However, recent clinical trials indicate an effective cure of hyperthyroidism with a relatively low incidence of hypothyroidism using individualised dosimetry [3–6].

From the radiation protection point of view, radioiodine therapy should be optimised in order to obtain the desired effect on the patient while keeping the absorbed dose as low as reasonably achievable (ALARA principle). Optimization and individualization of the administration of radioactivity for therapeutic purposes have been recommended by many scientific organizations [7,8], and the latest Euratom Directive 59/13 states that optimization and individualization are mandatory for the medical exposure of patients for any radiotherapeutic purpose [9]. Thus, it is imperative to provide an individualised calculation of radioiodine ^{131}I activity, as is the use of suitable methods to determine the optimum amounts of ^{131}I to administer.

There is an urgent need to introduce new tools to decrease

* Corresponding author.
E-mail address: jesusm.melgar.sspa@juntadeandalucia.es (J. Melgar Pérez).

https://doi.org/10.1016/j.ejmp.2019.04.026
Received 28 March 2018; Received in revised form 28 March 2019; Accepted 25 April 2019
Available online 06 May 2019

uncertainties in internal dosimetry with radiopharmaceuticals, as the availability of resources (personnel, time, and patient availability) remains limited in many nuclear medicine facilities. In addition, when a clinical dosimetry procedure is implemented, uncertainties should be considered for every patient [10].

In the pharmaceutical industry, an important drug development tool is population modelling [11–13]. Population models are used to identify and describe relationships between the physiological characteristics of subjects and the observed exposure or response to medications through statistical and mathematical methods [11–13]. This approach allows the characterization of the kinetics of a compound in a population with a limited number of measurements [11–13]. The application of this method to internal dosimetry results in more reliable estimates of the calculations and the quantification of uncertainties [14–19]. The term *population* does not imply that the individual patient is ignored. Individual data allow the description of variability and contribute to the identification of changes in drug exposure with changing individual parameters such as age, weight, and so forth [12]. From population modelling, individual biokinetic parameters and the subsequent absorbed dose estimation can be optimised by using Bayesian forecasting approaches [14–16]. Bayesian approaches are based on the inclusion of a priori information (as population parameters) in the fitting process of the biokinetic parameters for a new individual [13]. It has been shown that using this approach may be used to reduce the number of samples required in statistical estimation procedures [15].

The “gold standard” population method in biokinetics is the nonlinear mixed-effects model [11,16]. In statistics, when the investigator controls the level of a factor, the factor is fixed. If the investigator randomly samples the levels of a factor from a population, the factor is random. A mixed model is a statistical model containing both fixed and random effects. In the study of populations, it can be assumed that population parameters would be fixed factors, while individual parameters would be random factors [20]. In biokinetics, fixed-effects parameters represent the mean values of pharmacokinetic parameters in the population, and they are unknown constants to be determined [11–13,21]. Random effects quantify interindividual kinetic variability and residual variability. Interindividual kinetic variability represents the differences among parameters of different patients in the study population [11–13,21]. Residual variability represents the difference between the predicted values by the model and the observed values due to intra individual random variability: experimental errors, sampling error, and model selection [11–13,21]. The identification of the factors contributing to these variabilities and the exploration of their correlation with fixed effects are usually important components in population studies [11–13,21]. Mathematically, random effects are modelled as random variables assuming certain conditions. Nonlinear mixed-effects modelling can be used to obtain all parameter values (fixed and random effects) in a single stage, which, with few data per individual, can be fitted [11–13,21]. With this approach, population parameter values are estimated through the simultaneous operation of all individual data [11–13,21]. Moreover, the biokinetic individual data may be scarce, different between individuals, or have irregular sampling times [11–13,21]. To date, there are very few papers on the use of nonlinear mixed-effects modelling in radioiodine dosimetry [14–16]. These works used a large amount of data to build the model, from 4 to 12 measurements per patient, but in nuclear medicine facilities, hardly more than three measurements are taken per patient.

The objective of this work was to design and validate a population model applied to radioiodine biokinetics in patients with Graves’ disease using a nonlinear mixed-effects approach and three samples per patient. Scarce input data may produce a large bias in the estimation of the model parameters, but this also allows for the evaluation of the performance of this statistical tool under suboptimal conditions similar to real practice clinical conditions. Obtaining a validated model would allow the following:

1. Determination of population mean values and interindividual and residual variabilities.
2. An enhanced accuracy in the absorbed dose calculations for individualised therapy with ^{131}I [14–16].
3. Collection of fewer measurements from patients [14–16].
4. Prediction of unknown or missed observations.
5. Completion of patient data if, for any reason, they could not be properly obtained.

2. Materials and methods

^{123}I uptake values from 58 patients (39 women and 19 men; mean age [48 ± 12] years; range [26–85] years) who received radioiodine treatment for Graves’ disease in our center were used to build the population biokinetic model. ^{123}I uptake values were used to determine the optimal activity of ^{131}I to administer to patients. The protocol implemented is described below.

2.1. Dosimetric method

The dosimetric method used was previously described by Matheoud et al. [22], with some changes. Thyroid size and iodine biokinetic parameters were retrieved from planar scintigraphic images at 4, 24, and 96 h after injection of 111 MBq of ^{123}I. The acquisition time was 5 min for the first two acquisitions (at 4 and 24 h) and 10 min for the last acquisition. Planar scintigraphic imaging at 4 h was used to confirm hyperthyroidism.

Because therapy with ^{131}I liquid is administered orally, matching with the last measurement (at 96 h) taken from ^{123}I, patients visit the hospital a total of three times (one more time than using the fixed activities procedure). Absorbed dose values estimated from ^{131}I were not carried out. As verification, the decay-corrected uptake values between the two radioisotopes were compared in a few patients at 24 h post-administration. Antithyroid medication was stopped 10 days before the treatment. A total of 370 MBq of ^{131}I liquid was requested to enable a customised activity for Graves’ disease, and it was the highest activity administered to the patients.

The images were acquired with a dual gamma camera (Siemens-E CAM, Siemens Healthcare, Erlangen, Germany) equipped with a plane-parallel low-energy collimator, high resolution, two detectors, and a 256 × 256 matrix size. The administered activity measurement was carried out using an activimeter (Veenstra model VLB-202, Comecer Netherlands, Joure, the Netherlands).

Calculation of the therapeutic activity of radioiodine ^{131}I was carried out using the medical internal radiation dose (MIRD) approach. The MIRD formula for the absorbed dose, D_{MIRD}, in the thyroid, T, following the new nomenclature [23] is as follows:

$$D_{MIRD}(T, \infty) = \widetilde{A}(T, \infty)S(T \leftarrow T) \quad (1)$$

$$\widetilde{A}(T, \infty) = \int_0^{\infty} A(T,t)\, dt \quad (2)$$

where D_{MIRD} (T, ∞) is the mean absorbed dose in the thyroid, $\widetilde{A}$ (T,∞) is the time-integrated radioiodine activity in the thyroid, S(T← T) is the absorbed dose per unit of activity, and A (T, t) is the activity in the thyroid at time t.

Derived by a bicompartmental model [22], the following analytical formula is used to describe thyroid iodine uptake over time (U(t)), which enables calculation of $\widetilde{A}$ (T,∞):

$$U(t) = -\frac{U_0 k_a}{(k_a - k_e)}(\exp(-k_a t) - \exp(-k_e t)) \quad (3)$$

where U_0 is the fraction of iodine that is transferred to the thyroid or the maximum fractional thyroid uptake, k_a is the rate of biologic intake or absorption (the most important term when $t < T_{max}$, where T_{max} is the time of maximum activity), and k_e is the rate of biological clearance

or elimination (the most important term when $t > T_{max}$). As k_e is two orders of magnitude smaller than k_a, Eq. (3) is always defined.

In Eq. (3), we consider only biologic parameters (decay-corrected activity data) because ^{123}I is used for determining kinetics in patients, and ^{131}I is used for therapy.

As $A(T, t) = A_0U(t)$, where A_0 is the administered activity, and $k_e = \frac{\ln 2}{T_{e,b}}$, where $T_{e,b}$ is the biological half-life, the integration of (2) is given by:

$$\widetilde{A}(T, \infty) = \frac{A_0U_0}{k_e} = \frac{A_0U_0T_{e,b}}{\ln 2} \quad (4)$$

To calculate the therapeutic activity to obtain the planned absorbed dose, we must consider the physical half-life of ^{131}I. Thus, we replace biologic half-life ($T_{e,b}$) with effective half-life (T_{eff}) in (4), and the final expression for time-integrated radioiodine activity in the thyroid is:

$$\widetilde{A}(T, \infty) = \frac{A_0U_0T_{eff}}{\ln 2} \quad (5)$$

The effective half-life is defined as $T_{eff}^{-1} = T_{phys}^{-1} + T_{biol}^{-1}$, where T_{phys} is the physical half-life of ^{131}I and T_{biol} is the biological half-life, which is estimated from the analysis of planar scintigraphic images obtained using ^{123}I.

Thus, from (1) and (5), and considering the thyroid as the ellipsoid of rotation, where the S factor is 2.7/mass (Gy/MBqd) [22] and mass is expressed in grams, the activity to obtain the desired absorbed dose can be expressed as:

$$A_0(MBq) = 0.256\frac{D(Gy)\ m(g)}{U_0T_{eff}(d)} \quad (6)$$

Activities were calculated for a prescribed absorbed dose of 120 Gy. Changes in thyroid mass were not taken into account after therapeutic activity administration.

Biological uptake values (decay-corrected data) were obtained from scintigraphic images using ^{123}I. The gamma camera calibration factor (cps/MBq) was measured with syringes of different volumes located inside the neck phantom® (Biodex Medical System, New York, USA). The activities used were of 111 MBq.

The volumes selected were 2, 6, 10, 14, 20, and 40 mL. The center of the syringe was placed 3.5 cm from the surface of the phantom. This depth corresponds approximately to the mean value of the range of effective thyroid depths of hyperthyroid patients (2–5 cm) [24].

The relationship between the gamma camera calibration factor and the volume of the syringe was adjusted to a quadratic function. In this way, the calibration factor used in each patient was different and depended on the estimated thyroid volume, which thus represented a method for scattered radiation compensation.

Attenuation correction was not performed, but we estimated the bias of the calibration factor. The differences in the calibration factors were +16% at a 2-cm depth and −9% at a 4.7-cm depth with respect to the reference depth.

Biological uptake values were calculated from the gamma camera calibration factor and the region of interest (ROI) and background on planar images of the neck.

The ROI was delineated by a threshold of 40% of the maximum value of the values in the image. This threshold was obtained by comparing the actual dimensions of the syringes with those obtained in the planar images during the calibration process. The differences between the actual and estimated volumes of the syringes were less than 10%.

The background was drawn on a region close to the subclavian vessels and normalised to the size of the ROI. The Siemens Syngo MI Applications VB10B software® (Siemens, Erlangen, Germany) allows users to semi automatically draw the ROI and the background.

Uptake values at times t_i (i = 1,2,3; t_1 = 4 h, t_2 = 24 h y t_3 = 96 h) were calculated as follows:

$$U(t_i) = \frac{(C_{ROI} - C_{BKG})}{CF(V)A_{patient}} \exp(\lambda_{fis}t_i) \quad (7)$$

where C_{ROI} is the count rate in the ROI, C_{BKG} is the counts rate in the background normalised to the nodule ROI size, CF(V) is the volume-dependent gamma camera calibration curve obtained from the neck phantom, $A_{patient}$ is the activity of ^{123}I injected, and exp ($\lambda_{fis}t_i$) is the radioactive decay correction.

Because each patient provides three pairs of data, (t_i, U (t_i)), the parameters in Eq. (3) can be uniquely determined. As a quality control measure, the number of pixels in the ROI on the images acquired at 24 and 96 h was verified and did not differ by more than 2% from the ROI obtained during the acquisition at 4 h. If this value was exceeded, the threshold of the images was adjusted, and then the range of thresholds taken was [37–45%]. At 96 h, the mean number of counts in the ROIs of the patients was 11,000, and the signal-to-background ratio was 5:1.

In five patients, it was verified that the uptake values of ^{131}I were up to 10% lower than those of ^{123}I at 24 h after administration. Decay-corrected uptake values of ^{131}I were obtained following the described method but using a high-energy collimator.

The thyroid is considered a rotating ellipsoid with a and b as the vertical and horizontal axes with dimensions expressed in centimeters; assuming the density is 1 g/mL, the functioning mass is then $\pi ab^2/6$. The estimated average thyroid mass was 25 ± 17 g (24 ± 15 g for women and 28 ± 22 g for men). More details about this method can be found in our previous work [25].

2.2. Statistical modelling

A nonlinear mixed-effects model was used to characterize the iodine biokinetics in the study population. The rate of biologic intake is always two orders of magnitude higher than the rate of biologic clearance [26]; thus, the relationship (3) can be approximated as:

$$U(t) = -U_0(exp(-k_at) - exp(-k_et)) \quad (8)$$

where U_0, k_a, and k_e represent the level of uptake, rate of biologic intake, and rate of biologic clearance, respectively.

Eq. (8) represents the basic structural model, or systematic component, that describes the system. In addition to the systematic component, we must consider the system random components, or noise. Random components are described by a statistical model called a variance model [13].

We studied 58 patients and 174 (58 times 3) uptake values, so the observed uptake U_{ij} for patient j (j = 1…58) at time i (i = 1, 2, 3) becomes:

$$U_{ij} = -U_{0\_j}(\exp(-k_{a\_j}t_i) - \exp(-k_{e\_j}t_i)) + \varepsilon_{ij} \quad (9)$$

where U_{0_j} is the maximum fractional thyroid uptake for patient j; k_{a_j} is the intake rate for patient j; k_{e_j} is the clearance rate for patient j; t_i (i = 1,2,3), where t_1 = 4 h, t_2 = 24 h, or t_3 = 96 h represents the time elapsed after the administration of radioiodine; and ε_{ij} is the residual variability, residual error, or intrapatient variability that is modelled as a random variable.

Constant rates must be positive, so we applied natural logarithms: $k'_{a\_j} = \log k_{a\_j}$ and $k'_{e\_j} = \log k_{e\_j}$. This reparameterization is used for fitting the nonlinear mixed-effects model without constraints [21]. Thus,

$$U_{ij} = -U_{0\_j}(\exp(-\exp(k'_{a\_j})t_i) - \exp(-\exp(k'_{e\_j})t_i)) + \varepsilon_{ij} \quad (10)$$

To introduce fixed and random effects in a nonlinear mixed-effects model, we can rewrite the relationship (10) as follows:

$$U_{ij} = -(\bar{U}_0 + (U_{0\_j} - \bar{U}_0))\ [\ \exp(-\exp(\bar{k}'_a + (k'_{a\_j} - \bar{k}'_a))t_i) - \exp(-\exp(\bar{k}'_e + (k'_{e\_j} - \bar{k}'_e))t_i)] + \varepsilon_{ij} \quad (11)$$

where $\bar{U}_0$, $\bar{k}'_a$, $\bar{k}'_e$ represent the mean values (in log base the last two) of

the parameters in the population of patients. These terms are called fixed effects.

In the mixed-effects model, the deviations of individual values from the mean value of the coefficients (the fixed effects) are considered random effects, treating the patients as a sample from a population. Thus, $\alpha_{1j} = U_{0\_j} - \bar{U}_0$, $\alpha_{2j} = \bar{k}'_{a\_j} - \bar{k}'_2$, $\alpha_{3j} = \bar{k}'_{e\_j} - \bar{k}'_e$, where ($\alpha_{1j}$, α_{2j}, α_{3j}) represents interindividual variability or between-subject variability with random variables. We denoted these variables as the array $\boldsymbol{\alpha_j}$.

The relation (10) can be written as:

$$U_{ij} = -(\bar{U}_0 + \alpha_{1j}))\,[\exp(-\exp(\bar{k}'_a + \alpha_{2j})t_i) - \exp(-\exp(\bar{k}'_e + \alpha_{3j})t_i)] + \varepsilon_{ij} \quad (12)$$

The assumptions of this model are as follows: a) fixed effects are represented by $\vec{U}_0$, $\bar{k}'_a$, $\bar{k}'_e$ and b) random effects of interindividual variability are expressed as the matrix $\boldsymbol{\alpha_j}$ with j = 1…58. The random effects are modelled as multivariate normal (N), with mean **0** and variance-covariance matrix $\boldsymbol{\Psi}$, and are independent between patients and independent of the residual variability. The variance-covariance matrix $\boldsymbol{\Psi}$ is assumed to be symmetric and positive semidefinite; that is, all of its eigenvalues must be nonnegative. This condition simplifies the calculations for obtaining model parameter values [21]. Thus,

$$\boldsymbol{\alpha_j} \sim N(0, \begin{pmatrix} \psi_{11}^2 & \psi_{12}\psi_{13} \\ \psi_{21}\psi_{22}^2\psi_{23} & \\ \psi_{31}\psi_{32}\psi_{33}^2 & \end{pmatrix})$$

c) Residual variability ε_{ij} represents the measurement error and has the same statistical properties for all patients. This error is assumed to be independent of the measure, patient, and time, and it shows a normal distribution with mean 0 and variance σ^2.

Model parameter values were estimated with the maximum-likelihood method using Lindstrom and Bates' algorithm [21,27], which was implemented in the *nlme* function (linear and nonlinear mixed-effects models) of the R statistical environment (R Core Team 2014). This algorithm and *nlme* function are detailed in several previous articles [21,27].

The general model was compared with a model diagonal covariance-variance matrix (independent random effects) using the Akaike information criterion (AIC) [21] and the Bayesian information criterion (BIC) [21].

These information criterion statistics are defined from the logarithm of the likelihood function L as:

$$AIC = -2\log(L) + 2n_{par} \quad (13)$$

$$BIC = -2\log(L) + n_{par}\log(N) \quad (14)$$

where n_{par} denotes the number of parameters in the model and N denotes the total number of observations used to fit the model. Under these definitions, lower values are better.

AIC and BIC reward goodness of fit but also include a penalty that increases when the number of estimated parameters increases. The penalty discourages overfitting. To ensure statistical significance, a likelihood ratio test [21] was used to select the "best" model. This test is a statistical test of the goodness of fit between two nested models. A more complex model is compared with a simpler model to see if it fits a particular dataset significantly better. The null hypothesis is that the smaller model is the "best" model; if the null hypothesis is rejected, then the larger model is a significant improvement over the smaller one.

Once the model was selected, to take into account the possible relationship between the biokinetic parameters and the patients' three covariates (i.e., age, sex, and thyroid mass), we evaluated the scatter plot of the data (biokinetic parameters versus covariates) and added these covariates to the model. In pharmacokinetics, a covariate is any variable that is specific to an individual and may influence the pharmacokinetics of a drug. Thus, if a covariate is added to the model, the model may be enhanced.

2.3. Statistical model validation

The validity of the model assumptions was assessed using the Kolmogorov-Smirnov test [28], Bartlett's test [29], and diagnostic plots representing standardised values versus fitted values and sample quartiles versus theoretical quartiles.

We calculated the root mean squared error (RMSE) of the uptake values to verify the goodness of fit of the statistical model. The predictive power of the model was evaluated using the leave-one-out cross-validation (LOOCV) method. In the LOOCV method, an observation is removed, and then the model parameters are fitted again (with all observations less the removed observation), and the removed observation is predicted using the parameters of the new model. This procedure was repeated for each observation (a total of 174 times). These predictions are named "out-of-sample" predictions, while the predictions of observations that are part of input data of the model are named "in-sample" predictions. Predictions of observations were made using the empirical best linear unbiased prediction method [21,27], which was implemented in the R statistical environment [30]. The total number of predictions is lower than 174 for a lack of convergence of the maximum-likelihood algorithm to fit the model to some datasets.

The differences between observed uptake values and out-of-sample predicted values were measured using the root mean squared error of prediction (RMSEP). In this case, $RMSEP_{uptake}$ was calculated according to:

$$RMSEP_{uptake} = \sqrt{\frac{\sum_{j=1}^{N_j}\sum_{i=1}^{N_i}(U_{ij,obs} - U_{ij,pred}^{-ij})^2}{N}} \quad (15)$$

where $U_{ij,obs}$ is the observed uptake value in the j^{th} individual at the i^{th} time, $U_{ij,pred}^{-ij}$ is the predicted uptake value in the j^{th} individual at the i^{th} time, N_j is the total number of patients, N_i is the predicted uptake points number in the patients, and N is the total number of predicted observations.

Note that $RMSEP_{uptake}$ is a metric to evaluate the quality of prediction of unknown values (we "guess" the left-out observation by a model built on the kept observations) while RMSE evaluates how close the "predicted" value by the model is to the observed value but using as input data (for building the model) of all observed values. The RMSE and $RMSEP_{uptake}$ were calculated as a function of ^{123}I uptake time point (4, 24, and 96 h).

In addition, we evaluated the error in the calculations of the ^{131}I activity to administer when one measured ^{123}I uptake value is replaced by the (out-of-sample) predicted ^{123}I uptake value. Thus, when an observation was removed, we predicted the eliminated observation using our newly fitted model and then obtained new individual biokinetic parameter values and a new therapeutic activity to administer. This new therapeutic activity to administer was named "predicted activity."

The differences between the "predicted" activities and "real" activities (calculated activities from measured ^{123}I uptake values) were measured using the following expression for $RMSEP_{activity}$:

$$RMSEP_{activity} = \sqrt{\frac{\sum_{j=1}^{N_j}\sum_{i=1}^{N_i}(A_{j,obs} - A_{ij,pred}^{-ij})^2}{N}} \quad (16)$$

where $A_{j,obs}$ is the calculated activity of ^{131}I in the j^{th} patient and $A_{ij,pred}^{-ij}$ is the predicted activity of ^{131}I from the dataset for the j^{th} patient and the i^{th} replaced observation. $RMSEP_{activity}$ was calculated as a function of ^{123}I uptake time point (4,24, and 96 h).

Plots and statistical parameters were calculated using the R statistical environment [30], and metrics were calculated using a spreadsheet.

3. Results

Table 1 shows the AIC, BIC, and Log (L) values of the two models,

Table 1
Comparison of the general model versus independent random effects model.

Model	AIC	BIC	Log (L)
General	–391.7	–360.1	205.9
Independent random effects	–317.6	–295.5	165.8

Likelihood ratio test ($p < 0.0001$).

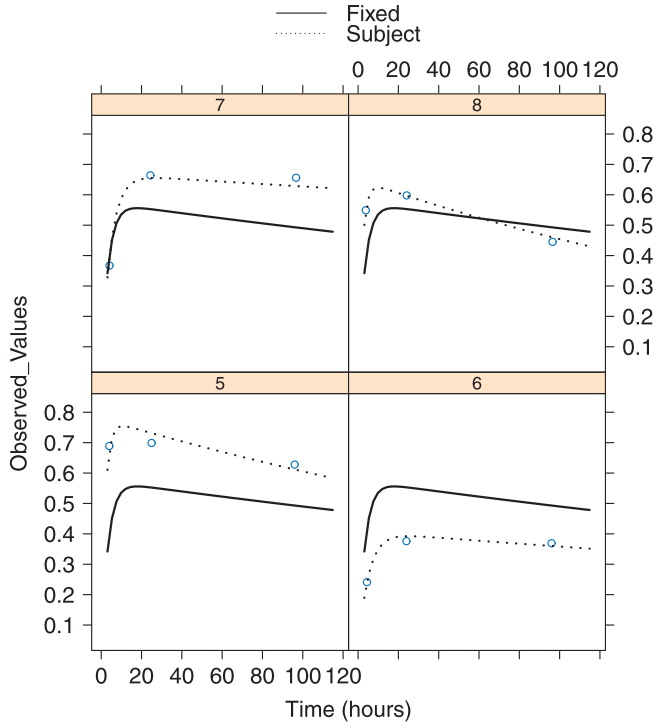

Fig. 1. Observed biologic uptake values after decay correction for ^{123}I (points), individual uptake curve (dotted line), and average population curve (solid line) estimated from nonlinear mixed-effect modelling for four patients.

that is, the general model (variance/covariance matrix is positive-definite and symmetric) and independent random-effects model (variance/covariance matrix is diagonal).

A lower AIC or BIC value indicates a better fit. As shown in Table 1, the general model was selected.

Fig. 1 shows the observed uptake values after decay correction for ^{123}I (points) versus time (hours) for four patients. The individual uptake curve (dotted line) and average population curve (solid line) were estimated from nonlinear mixed-effect modelling.

The addition of all covariates studied (age, sex, and thyroid mass) to the model either did not significantly enhance the fitting or the fit did not converge, and the examination of the scatter plot did not show any relationship between the biokinetic parameters and the covariates.

Estimates of the fixed and random effects are given in Tables 2 and 3, respectively. Fixed effects are shown with standard errors and their values in the original scale, that is, exp(mean value), which are named

Table 2
Fixed effects: estimated values and standard errors.

Variables	Estimated values	Standard error
$\bar{U}_0$	0.575	0.020
$\bar{k}_a'$	–1.221	0.056
$\bar{k}_e'$	–6.44	0.10
$\bar{k}_a (h^{-1})$	0.2949	—
$\bar{k}_e (h^{-1})$	0.0016	—

Table 3
Random effects: variance-covariance matrix, standard deviations, and correlations.

Variable	Values
Variance-covariance matrix (Ψ)	$\begin{pmatrix} \mathbf{0.020} & \mathbf{0.042} & \mathbf{0.021} \\ \mathbf{0.042} & \mathbf{0.133} & \mathbf{0.138} \\ \mathbf{0.021} & \mathbf{0.138} & \mathbf{0.221} \end{pmatrix}$
Residual standard deviation	0.029
Standard deviation (α_1)	0.14
Standard deviation (α_2)	0.36
Standard deviation (α_3)	0.47
Correlation (α_{12})	0.81
Correlation (α_{13})	0.31
Correlation (α_{23})	0.81

as $\bar{k}_a$ and $\bar{k}_e$

For random effects, the variance-covariance matrix, standard deviations of random effects (residual and interindividual variability), and correlations among random effects **α** are presented.

Diagnostic plots did not indicate serious departures from normality (not shown). The Kolmogorov-Smirnov test and Bartlett's test confirmed the normality and variance constancy of the residual error. The Kolmogorov-Smirnov test confirmed the normality of random effects.

Table 4 shows the RMSE of in-sample predictions of uptake values from the fitted model and the $RMSEP_{uptake}$ of out-of-sample predictions of uptake values from the LOOCV. RMSE and $RMSEP_{uptake}$ are shown as a function of ^{123}I uptake time point.

Table 5 shows $RMSEP_{activity}$ values of ^{131}I activities to administer as a function of uptake time point.

"Predicted" activities to administer were calculated from the out-of-sample predictions of uptake values of ^{123}I and the LOOCV. "Real"^{131}I activities to administer were taken from calculated activities of the measured uptake values of ^{123}I.

4. Discussion

In this work, a population biokinetic model for radioiodine in the thyroid of patients with Graves' disease was designed. In general, the assumptions of the model were verified, and only a few outliers appeared in the data.

The fixed effects, which represented the mean values of population biokinetic parameters obtained in this study, showed differences and similarities in relation to those obtained in other studies. Specifically, the estimated maximum fractional thyroid uptake (U_0) was similar to that found by Areberg et al. [16] and Jöhnson et al. [31] but different from that reported by Merrill et al. [14]. Otherwise, the effective half-life was similar to that found by Merrill et al. [14], Jönsson et al. [31], and Carlier et al. [32] but was 25% higher than that reported by Areberg et al. [16]. The rate of intake was 40% lower than that obtained by Areberg et al. [16] and Merrill et al. [14]. However, we should note that only Merrill et al. [14] and Areberg et al. [16] used a nonlinear mixed-effects model (see Table 6).

These differences can be explained several ways. First, the study populations are different because they correspond to different locations. In addition, we employed a model with additive error, as did Areberg et al. [16], while Merrill et al. [14] applied a multiplicative error. In addition, the procedures performed to acquire uptake values in the thyroid were distinct. Areberg et al. [16] used a thyroid uptake probe, and Merrill's data were obtained with an ionization chamber. Areberg et al. [16] included different varieties of hyperthyroidism, including diffuse goiter, multinodular goiter, and adenoma, while we included only Graves' disease patients. Areberg et al. [16] and Merrill et al. [14] included four and seven samples per patient, respectively, and these authors also used ^{131}I.

The developed statistical model included 10 parameters, and covariates were not included because correlations were not shown from the

Table 4
RMSE values of in-sample predictions and $RMSEP_{uptake}$ values of out-of-sample predictions (from the LOOCV) as a function of ^{123}I uptake time point.

Uptake time point	Number of in-sample predictions	RMSE (CV)	Number of out-of-sample predictions	$RMSEP_{uptake}$ (CV)
[4 h]	58	0.014 (3.3%)	58	0.079 (19%)
[24 h]	58	0.022 (4.1%)	55	0.039 (7.1%)
[96 h]	58	0.019 (3.8%)	56	0.053 (11%)
All	174	0.019 (3.8%)	169	0.059 (12%)

CV: coefficient of variation = RMSE or $RMSEP_{uptake}$/observed mean uptake value, expressed in percentages.

Table 5
$RMSEP_{activity}$ values of ^{131}I activities to administer derived from the out-of-sample predictions of uptake values of ^{123}I, as a function of uptake time point.

Uptake time point	Number of predictions	$RMSEP_{activity}$ (CV)
[4 h]	58	26 (10%)
[24 h]	55	22 (8.5%)
[96 h]	56	38 (15%)
All	169	30 (12%)

CV: coefficient of variation = $RMSEP_{activity}$/real mean activity, expressed in percentages.
Predicted activities were obtained from out-of-sample predictions of uptake values of ^{123}I from the LOOCV.
Real calculated activities were taken from the measured uptake values of ^{123}I.

plots between biokinetic parameter values and covariates. Our model is more complex than Areberg's and Merrill's basic models, which included seven parameters (diagonal variance-covariance matrix), although Areberg et al. [16] added more covariates to enhance the predictive accuracy of the model. However, our model was more practical because we included three samples per patient; moreover, the residual error was 0.0258, whereas Areberg et al. [16] obtained a value of 0.018 and Merrill et al. [14] obtained a value of 0.1156. Nevertheless, as the optimal number of samples to fit a curve for the kinetics of radioiodine thyroid uptake moves from five to eight [15], we must assume parameter estimates and predictions are biased [13]. In addition, our sampling time sequence to fit the uptake curve was not optimal. Merlé et al. [13], Merrill et al.[14], and Amato et al.[33] determined the optimal sampling time sequence for radioiodine therapy in Graves' disease and other benign thyroid diseases for three measured points. The sampling time sequences obtained were t = 1-12-296 h, t = 4-96-168 h, and t = 3(6)-24-168 h, respectively. In our case, as ^{123}I has a physical half-life of 13.2 h, it would be useless to perform acquisition images later than 96–120 h from administration (to achieve an acceptable signal-to-noise ratio).

Interindividual variability was 25% for uptake, 38% for intake rate, and 50% for clearance rate, compared with the values of 18%, 33%, and 59%, respectively, given by Areberg et al. [16] (model without covariates). It is remarkable that interindividual variabilities were similar in both studies because Areberg et al. [16] included seven times more patients than we did, which was likely due to the inclusion of all thyroid benign diagnoses in that study. Otherwise, Merrill et al. [14] reported interindividual variabilities greater than 100%. In this case, the dosimetric procedure and error modelling used could explain these differences. Thus, to obtain accurate uptake values, the calibration factor (activity/counts) must be corrected for scatter and source attenuation [24,34], but in practice, corrections are generally not made. In this work, a quadratic fit of the gamma camera calibration factor against the functioning volume (obtained from a neck phantom at an intermediate depth of measurement) was performed with the least squares method [25]; as a result, it is likely that interindividual variabilities were lower.

Another issue regarding methodology is the administration of ^{123}I instead of ^{131}I to predict thyroid kinetics. There are practical advantages involving the selection of ^{123}I with our protocol, such as the acquisition of all dosimetric parameters in the diagnostic phase, a reduction in the number of hospital visits (the patient makes only one additional medical visit), optimal image resolution, and the decrease in time elapsed between the diagnostic phase and therapy (4 days), whereby more reliable thyroid uptake values can be obtained [35]. In addition, the agreement of the uptake values between the two isotopes must be compared. Canzi et al. [26] reported high correlations among dosimetric parameters obtained with each isotope (0.88 for maximum uptake and 1.01 for effective half-life of clearance), and in a previous work [25], we verified this agreement in a select number of patients for the uptake at 24 h after radioiodine administration. It is true that at 96 h, the scintigraphic image is noisy and the measurement not sufficiently late for high-accuracy estimates of the effective half-life. Willegaignon et al. [36] reported a deviation mean of 13 ± 11% between the effective half-life of clearance calculated by considering a set of six measured points (2-6-24-48-96-220 h) against a set of two points (24–96 h) after radioiodine administration. Matheoud et al. [22] found deviations ranged between −14% and 13% with a set of three measured points (4–24-120 h). Amato et al. [33] reported a mean deviation of 1 ± 15% between therapeutic activity calculated with a set of six measured points (3-6-24-48-72/96-168 h) against a set of three points (3-24-96 h). Thus, in our case, taking an uncertainty of 15% (for not including another measurement later than 96/120 h) and assuming a measurement uncertainty of 20% at 96-h measurement, the impact on dose assessment is lower than 25%.

Based on all of these results, we believe that ^{123}I data and ^{131}I data could be similar or, at least, the performance of this tool and the results obtained should be analogous to that using input data obtained with ^{131}I. However, it is true that in order to achieve a full verification of all methos described (specially using ^{123}I instead ^{131}I), is necessary to use or compare with ^{131}I data.

Because of the described limitations of ^{123}I as a radiotracer in radioiodine therapy, we sought to investigate new tools to increase the accuracy of the absorbed dose estimates in thyroid therapy. The applied dosimetric method in our center seeks a compromise among the accuracy of the calculations, the consumption of resources, and patient comfort.

The correlation between the observed and fitted uptake values was

Table 6
Population biokinetic parameter values in the literature.

Study	Maximum uptake (%)	Elimination effective rate (days)	Intake rate (%)
Areberg et al. [16]	53	4.2	0.4055
Merrill et al. [14]	79	5.3	0.4142
Jönsson et al. [31]	63	5	—
Carlier et al. [32]	—	5.1	—
Present study	57.5	5.6	0.295

very high (RMSE = 4%), and the thyroid uptake could be estimated with a low uncertainty (residual variability = 3%).

The predictive performance of the model, which was evaluated by $RMSEP_{uptake}$, was 12% using the LOOCV procedure. The $RMSEP_{uptake}$ was lower for the uptake value at 24 h (7%) and higher for the uptake value at 4 h (18%). These results can be intuitively understood, as there were measuring points with higher weight than others in the model. Merlé et al. [15] studied this problem, applying the concept of Shannon information. These authors concluded, from 12 data points per patient (1-2-4-6-12-24-48-72-96-168-192-216 h) from 101 patients, that the optimal sampling time sequence was 2 h for a 1-point schedule and 2 and 168 h for a 2-point schedule. Our results are consistent with these conclusions, as lower $RMSEP_{uptake}$ values corresponded with the earlier measurement and the latest measurement for the 2-point schedule, and a higher $RMSEP_{uptake}$ was calculated when the first measurement was removed.

The $RMSEP_{activity}$ was 12%. In this case, the last measurement (96 h) was the most important (the $RMSEP_{activity}$ was higher when this measurement was eliminated). This result is coherent with that of Merrill et al. [14], who reported that the optimal time with the 1-point schedule was the last sample (168 h) for calculation of integrated-time activity. The importance of the late uptake measurement has also been discussed by other authors [33,37,38].

An important fact to highlight is that we evaluated the error involved in making predictions by the model and the derived errors in the calculations. Merrill et al. [14] measured the uncertainty of the biokinetic parameters obtained through the resampling of their data (bootstrapping), but they did not evaluate the predictive ability of out-of-sample observations.

Mixed-effects modelling is a very practical tool because population biokinetic parameter values can be calculated in a one-stage approach, where it is not necessary to obtain individual parameter values initially and the accuracy of individual biokinetic parameter values can be enhanced. Moreover, model parameters can be calculated with unbalanced data, missing values, and few samples per patient.

The calculation time for all parameters depends of the choice of initial values. In our case, we used a heuristic procedure, but there are simpler procedures [21]. A desktop computer took 9 s to obtain the model parameter values (four cores at a 3.4-GHz frequency).

The implemented tool enabled us to classify sampling schedules for the thyroid uptake curve as a function of predictive accuracy, which could be used to select the optimal schedule according to the time and resources of the center. For example, we could use a 2-point schedule with two measurements (4 and 96 h) and to make the prediction of the 24-h measurement by the model, because the 3-point sequence had an RMSE of 4%, and the previous 2-point schedule (together with the prediction of the 24-h measurement) had an $RMSEP_{activity}$ of 8.5%. This finding is consistent with those of Merrill et al. [14] and Merlé et al [15], showing that a third measurement provides a small additional improvement.

The building of the population biokinetic model initially requires a large amount of patient data, but unlike other papers, we evaluated the performance of this statistical tool in non ideal conditions (with three samples per patient), which is more in line with that obtained in clinical practice.

In addition to delivering the optimal absorbed dose to the thyroid, it would be beneficial to know whether the individualization of radioiodine ^{131}I therapy could produce better clinical outcomes. Previous studies seem to show positive evidence for individualization. Schiavo et al. [5] showed an effective cure of toxic multinodular goiter with relatively low ^{131}I activities and a low incidence of hypothyroidism. Rokni et al. [6] performed a *meta*-analysis with two randomised and five nonrandomised studies and concluded that the calculated activity (individualised method) may be superior to the method of fixed activities in patients diagnosed with toxic multinodular goiter. Therefore, it is reasonable to use such methods to enhance and simplify individualised dosimetry in hyperthyroidism from a clinical perspective.

Mixed-effects modelling may be used in several fields of biokinetic and radiation dosimetry. In radionuclide therapy, this tool could be useful to generate realistic time-activity curves and enhance Monte Carlo simulations of acquisitions in therapeutic procedures [39–41]. In oncology, this approach can be used to model tumour volume and tumour regrowth kinetics [42–45] or to predict treatment outcomes in chemoradiotherapy and/or radiotherapy [46,47]. Furthermore, these models could be used to optimise the absorbed dose as a function of patient-specific variables and to enhance treatment outcomes.

5. Conclusions

This work applies a general methodology to model and validate iodine kinetics using a population-based and mixed-model approach. This type of modelling can improve the accuracy and precision of biokinetic parameter values included in the formulation of MIRD guidelines to calculate individualised activity. The current model was built from only three samples per patient, which suggests that it could be applied in routine clinical practice.

Three important features of the present tool were demonstrated: speed of calculation, flexibility, and high predictive ability. Thus, model parameters were obtained with a conventional computer in a few seconds. Moreover, the estimation of model parameters could be carried out with unbalanced data, missing values and few samples per patient. The fitted model predicted with high accuracy both observed uptake values and new observations.

The predictive ability of this model enables quantification of the accuracy of different time-sampling sequences of the radioiodine thyroid uptake curve. Consequently, each department of nuclear medicine could determine their optimal work protocol as a function of time, organization, and resources. In our case, we could change from the 3-point schedule (4, 24, and 96 h) to a 2-point schedule (4 and 96 h) with a limited loss of accuracy, as other authors have reported. A final verification of the described methods will require using ^{131}I data. Applications of the mixed-effects model are general and could be extended to other areas of biokinetics and radiation dosimetry.

References

[1] De Rooij A, Vandenbroucke JP, Smit JW, Stokkel MP, Dekkers OM. Clinical outcomes after estimated versus calculated activity of radioiodine for the treatment of hyperthyroidism: systematic review and meta-analysis. Eur J Endocrinol 2009;161:771–7.

[2] Bernard D, Desruet MD, Wolf M, Roux J, Boin C, Mazet R, et al. Radioiodine therapy in benign thyroid disorders. Evaluation of French nuclear medicine practices. Ann Endocrinol (Paris) 2014;75:241–6.

[3] Zakavi SR, Mousavi Z, Davachi B. Comparison of four different protocols of I-131 therapy for treating single toxic thyroid nodule. Nucl Med Commun 2009;30:169–75.

[4] Traino AC, Xhafa B. Accuracy of two simple methods for estimation of thyroidal 131I kinetics for dosimetry-based treatment of Graves' disease. Med Phys 2009;36:1212–8.

[5] Schiavo M, Bagnara MC, Camerieri L, Pomposelli E, Giusti M, Pesce G, et al. Clinical efficacy of radioiodine therapy in multinodular toxic goiter, applying an implemented dose calculation algorithm. Endocrine 2015;48:902–8.

[6] Rokni H, Sadeghi R, Moossavi Z, Treglia G, Zakavi SR. Efficacy of different protocols of radioiodine therapy for treatment of toxic nodular goiter: systematic review and meta-analysis of the literature. Int J Endocrinol Metab 2014;12:e14424.

[7] International Commission on Radiological Protection. Recommendations of the International Commission on radiological protection. ICRP Publication 26. Ann ICRP 1(3); 1977.

[8] International Commission on Radiation Units and Measurements. Absorbed-Dose Specification in Nuclear Medicine. Report n.67. Ashford, England: Nuclear Technology Publishing; 2002.

[9] European Council Directive 2013/59/Euratom on basic safety standards for protection against the dangers arising from exposure to ionising radiation and repealing Directives 89/618/Euratom, 90/641/Euratom, 96/29/Euratom, 97/43/Euratom and 2003/122/Euratom. OJ of the EU 2014 L13; 57:1–73.

[10] Lassmann M, Chiesa C, Flux G, Bardiès M. EANM Dosimetry Committee guidance document: good practice of clinical dosimetry reporting. Eur J Nucl Med Mol Imaging 2011;38(1):192–200.

[11] U.S. Department of Health and Human Services, Food and Drug Administration, Center for Drug Evaluation and Research, Center for Biologics Evaluation and Research. Guidance for industry population pharmacokinetics. https://www.fda.gov/downloads/drugs/guidances/UCM0721 37.pdf [Accessed 1 February 2018].
[12] Mould DR, Upton RN. Basic concepts in population modeling, simulation, and model-based drug development. CPT Pharmacometrics Syst Pharmacol 2012;1(9):e6.
[13] Bonate P. Pharmacokinetic-pharmacodynamic modeling and simulation. New York: Springer Science + Business Media; 2006.
[14] Merrill S, Horowitz J, Traino AC, Chipkin SR, Hollot CV, Chait Y. Accuracy and optimal timing of activity measurements in estimating the absorbed dose of radioiodine in the treatment of Graves' disease. Phys Med Biol 2011;56:557–71.
[15] Merlé Y, Mentré F, Mallet A. Designing an optimal experiment for bayesian estimation: application to the kinetics of iodine thyroid uptake. Stat Med 1994;13:185–96.
[16] Areberg J, Jönsson H, Mattsson S. Population biokinetic modeling of thyroid uptake and retention of radioiodine. Cancer Biother Radiopharm 2005;20:1–10.
[17] Hardiansyah D, Maass C, Attarwala AA, Müller B, Kletting P, Mottaghy FM, et al. The role of patient-based treatment planning in peptide receptor radionuclide therapy. Eur J Nucl Med Mol Imaging 2016;43(5):871–80.
[18] Maaß C, Kletting P, Bunjes D, Mahren B, Beer AJ, Glatting G. Population-based modeling improves treatment planning before (90) Y-labeled anti-CD66 antibody radioimmunotherapy. Cancer Biother Radiopharm 2015;30(7):285–90.
[19] Hardiansyah D, Attarwala AA, Kletting P, Mottaghy FM, Glatting G. Prediction of time-integrated activity coefficients in PRRT using simulated dynamic PET and a pharmacokinetic model. Phys Med 2017;42(Suppl. C):298–304.
[20] Lyman R, Longnecker M. An Introduction to Statistical Methods and Data Analysis. 6thed. Belmont, USA: Brooks/Cole; 2010.
[21] Pinheiro JC, Bates DM. Mixed-effects models in S and S-plus. New York, USA: Springer-Verlag; 2000.
[22] Matheoud R, Canzi C, Reschini E, Zito F, Voltini F, Gerundini P. Tissue-specific dosimetry for radioiodine therapy of the autonomous thyroid nodule. Med Phys 2003;30:791–8.
[23] Bolch WE, Eckerman KF, Sgouros G, Thomas SR. MIRD Pamphlet n. 21: a generalized schema for radiopharmaceutical dosimetry—standardization of nomenclature. Nucl Med 2009;50:477–84.
[24] Osko J, Golnik N, Pliszczynski T. Uncertainties in determination of 131I activity in thyroid gland. Rad Prot Dosim 2007;125:516–9.
[25] Melgar J, Orellana A, Santaella Y, Arrocha JF. Comparación dosimétrica entre actividad fija y actividad individualizada en el tratamiento de la enfermedad de Graves con 131I. Rev Fis Med 2013;14:123–30.
[26] Canzi C, Zito F, Voltini F, Reschini E, Gerundini P. Verification of the agreement of two dosimetric methods with radioiodine therapy in hyperthyroid patients. Med Phys 2006;33:2860–7.
[27] Lindstrom MJ, Bates DM. Nonlinear mixed effects models for repeated measures data. Biometrics 1990;46:673–87.
[28] Teetor P. R Cookbook.Sebastopol, USA. O'Reilly Media; 2011.
[29] Zuur AF, Ieno EN, Walker NJ, Saveliev AA, Mixed Smith GM. Effects models and extensions in ecology with R. New York, USA: Springer Science + Business Media; 2009.
[30] R Core Team. R: a language and environment for statistical computing. Vienna, Austria: R Foundation for Statistical Computing; 2014.
[31] Jönsson H, Mattsson S. Excess radiation absorbed doses from non-optimised radioiodine treatment of hyperthyroidism. Radiat Prot Dosim 2004;108:107–14.
[32] Carlier T, Salaun PY, Cavarec MB, Valette F, Turzo A, Bardiès M, et al. Optimized radioiodine therapy for Graves' disease: two MIRD-based models for the computation of patient-specific therapeutic 131I activity. Nucl Med Commun 2006;27:559–66.
[33] Amato E, Campennì A, Leotta S, Ruggeri RM, Baldari S. Treatment of hyperthyroidism with radioiodine targeted activity: a comparison between two dosimetric methods. Phys Med 2016;32(6):847–53.
[34] Kramer GH, Crowley P. The assessment of the effect of thyroid size and shape on the activitiy estimate using Monte Carlo simulation. Health Phys 2000;78:727–38.
[35] Hänscheid H, Canzi C, Eschner W, Flux G, Luster M, Strigari L, et al. Dosimetry committee series on standard operational procedures for pre-therapeutic dosimetry II. Dosimetry prior to radioiodine therapy of benign thyroid diseases. Eur J Nucl Med Mol Imaging 2013;40:1126–34.
[36] Willegaignon J, Sapienza MT, Filho GBC, Traino AC, Buchpiguel CA. Determining thyroid 131I effective half-life for the treatment planning of Graves' disease. Med Phys 2013;40:022502.
[37] Berg GEB, Michanek AMK, Holmberg ECV, Fink M. Iodine-131 treatment of hyperthyroidism: significance of effective half-life measurements. J Nucl Med 1996;37:228–32.
[38] Bockisch A, Jamitzky T, Derwanz R, Biersack HJ. Optimized dose planning of radioiodine therapy of benign thyroidal diseases. J Nucl Med 1993;34:1632–8.
[39] Sarrut D, Bardiès M, Boussion N, Freud N, Jan S, Létang JM, et al. A review of the use and potential of the GATE Monte Carlo simulation code for radiation therapy and dosimetry applications. Med Phys 2014;41:064301.
[40] Garcia M-P, Villoing D, McKay E, Ferrer L, Cremonesi M, Botta F, et al. Test Dose: a nuclear medicine software based on Monte Carlo modeling for generating gamma camera acquisitions and dosimetry. Med Phys 2015;42:6885–94.
[41] Costa GCA, Bonifacio DAB, Sarrut D, Cajgfinger T, Bardiès M. Optimization of GATE simulations for whole-body planar scintigraphic acquisitions using the XCAT male phantom with 177Lu-DOTATATE biokinetics in a Siemens Symbia T2. Phys Med 2017;42:292–7.
[42] Miles DR, Wada DR, Jumbe NL, Lacy SA, Nguyen LT. Population pharmacokinetic/pharmacodynamic modeling of tumor growth kinetics in medullary thyroid cancer patients receiving cabozantinib. Anticancer Drugs 2016;27(4):328–41.
[43] Zhang H, Hyrien O, Pandya KJ, Keng PC, Chen Y. Tumor response kinetics after schedule-dependent paclitaxel chemoradiation treatment for inoperable non-small cell lung cancer: a model for low-dose chemotherapy radiosensitization. J Thorac Oncol 2008;3(6):563–8.
[44] Bastogne T, Samson A, Vallois P, Wantz-Mézières S, Pinel S, Bechet D, et al. Phenomenological modeling of tumor diameter growth based on a mixed effects model. J Theor Biol 2010;262(3):544–52.
[45] Rashid M, Heikkonen J, Singh AD, Kivelä TT. Clinical predictors of regression of choroidal melanomas after brachytherapy: a growth curve model. Ophthalmology 2018;125(5):747–54.
[46] Mareschal J, Weber K, Rigoli P, Biason E, Frambati L, Gotteland C, et al. The ADAPP trial: a two-year longitudinal multidisciplinary intervention study for prostate cancer frail patients on androgen deprivation associated to curative radiotherapy. Acta Oncol 2017;56(4):569–74.
[47] Rosenthal DI, Mendoza TR, Fuller CD, Hutcheson KA, Wang XS, Hanna EY, et al. Patterns of symptom burden during radiotherapy or concurrent chemoradiotherapy for head and neck cancer: a prospective analysis using the University of Texas MD Anderson Cancer Center Symptom Inventory-Head and Neck Module. Cancer 2014;120(13):1975–84.